HHS Public Access

Author manuscript

Nat Genet. Author manuscript; available in PMC 2017 August 08.

Published in final edited form as:

Nat Genet. 2013 February ; 45(2): 186–190. doi:10.1038/ng.2508.

Exome sequencing identifies mutation in *CNOT3* and ribosomal genes *RPL5* and *RPL10* in T-cell acute lymphoblastic leukemia

Kim De Keersmaecker[1,2,9], **Zeynep Kalender Atak**[1,9], **Ning Li**[3,9], **Carmen Vicente**[1,2], **Stephanie Patchett**[4], **Tiziana Girardi**[1,2], **Valentina Gianfelici**[1,2], **Ellen Geerdens**[1,2], **Emmanuelle Clappier**[5], **Michaël Porcu**[1,2], **Idoya Lahortiga**[1,2], **Rossella Lucà**[1,2], **Jiekun Yan**[1,2], **Gert Hulselmans**[1], **Hilde Vranckx**[1], **Roel Vandepoel**[1,2], **Bram Sweron**[1,2], **Kris Jacobs**[1,2], **Nicole Mentens**[1,2], **Iwona Wlodarska**[1], **Barbara Cauwelier**[6], **Jacqueline Cloos**[7], **Jean Soulier**[5], **Anne Uyttebroeck**[8], **Claudia Bagni**[1,2], **Bassem A Hassan**[1,2], **Peter Vandenberghe**[1], **Arlen W Johnson**[4], **Stein Aerts**[1,9], and **Jan Cools**[1,2,9]

[1]Center for Human Genetics, KU Leuven, Leuven, Belgium [2]Center for the Biology of Disease, VIB, Leuven, Belgium [3]BGI Europe, Copenhagen, Denmark [4]Section of Molecular Genetics and Microbiology, Institute for Cellular and Molecular Biology, The University of Texas at Austin, Austin, Texas, USA [5]Hôpital Saint-Louis, Paris, France [6]AZ St-Jan, Bruges, Belgium [7]Pediatric Oncology/Hematology and Hematology, VU Medical Center, Amsterdam, The Netherlands [8]Pediatric Hemato-Oncology, University Hospitals Leuven, Leuven, Belgium

Abstract

T-cell acute lymphoblastic leukemia (T-ALL) is caused by the cooperation of multiple oncogenic lesions[1,2]. We used exome sequencing on 67 T-ALLs to gain insight into the mutational spectrum in these leukemias. We detected protein-altering mutations in 508 genes, with an average of 8.2 mutations in pediatric and 21.0 mutations in adult T-ALL. Using stringent filtering, we predict seven new oncogenic driver genes in T-ALL. We identify *CNOT3* as a tumor suppressor mutated in 7 of 89 (7.9%) adult T-ALLs, and its knockdown causes tumors in a sensitized *Drosophila melanogaster* model[3]. In addition, we identify mutations affecting the ribosomal proteins RPL5 and RPL10 in 12 of 122 (9.8%) pediatric T-ALLs, with recurrent alterations of Arg98 in RPL10. Yeast and lymphoid cells expressing the RPL10 Arg98Ser mutant showed a ribosome biogenesis

Correspondence should be addressed to S.A. (stein.aerts@med.kuleuven.be) or J. Cools (jan.cools@cme.vib-kuleuven.be).

[9]These authors contributed equally to this work.

Accession codes. Sequence and variant data are available from the European Genome-phenome Archive (EGA) under accession EGAS00001000296, and somatic variants are available through a BioMart interface at http://lcbmart.aertslab.org/.

Note: Supplementary information is available in the online version of the paper.

AUTHOR CONTRIBUTIONS

All authors contributed to the writing of the manuscript. K.D.K., Z.K.A., N.L., C.B., B.A.H. and A.W.J. designed and performed experiments and analyzed data. C.V. and J.Y. performed and analyzed *Not3 Drosophila* experiments. S.P. performed and analyzed *Rpl10* yeast studies. R.L. performed and analyzed polysome profiling experiments. T.G., V.G., E.G., M.P., I.L., G.H., E.C., R.V., B.S., K.J., N.M. and I.W. performed experiments and analyzed data. H.V., B.C., J. Cloos, J.S., A.U. and P.V. collected samples and analyzed data. S.A. and J. Cools supervised the project, designed experiments and analyzed data.

COMPETING FINANCIAL INTERESTS

The authors declare competing financial interests: details are available in the online version of the paper.

defect. Our data provide insights into the mutational landscape of pediatric versus adult T-ALL and identify the ribosome as a potential oncogenic factor.

T-ALL is a genetically heterogeneous leukemia that is caused by the accumulation of multiple oncogenic lesions, which have been identified through characterization of chromosomal aberrations or via candidate gene sequencing[4–7]. In addition, recent whole-genome sequencing of 12 immature early T-cell precursor (ETP) ALLs revealed several new oncogenic drivers in this T-ALL subtype[8]. To discover new disease-driving genes in pediatric and adult T-ALL, we performed exome sequencing on 67 diagnostic T-ALL samples, 39 matched remission samples and 17 T-ALL cell lines (Supplementary Tables 1–3 and Supplementary Note).

To identify somatic mutations, we limited our initial analysis to the 39 paired samples acquired in the same individual at diagnosis and remission. To assess the performance of variant calling, 185 predicted single-nucleotide variations (SNVs) were validated by Sanger sequencing. This set was used to determine the filtering strategy with the best sensitivity and specificity. Different parameters were tested as filters, including sequencing coverage of the variant nucleotide, variant allele frequency, variant quality and presence in repeat regions. Finally, ranging thresholds of the somatic score, as calculated by SomaticSniper[9], were used as a filter (Supplementary Fig. 1). Removing variants with a somatic score below 70 resulted in 89% sensitivity and 96% specificity. Using this filter, a second batch of SNVs was selected for testing with capillary sequencing, which confirmed 80% (67 of 84) of the predicted SNVs.

We identified 1,810 somatic SNVs and 1,248 insertion and/or deletions (indels) in the 39 diagnostic-remission pairs. Excessively high numbers of somatic indels were present in three samples, possibly owing to defective DNA repair. These indels were excluded from candidate gene detection. One-fourth of the somatic mutations were protein altering, with the majority being missense mutations (413); the rest were frameshift indels (55), in-frame indels (30), nonsense coding (32) or splice-site mutations (39). On average, each sample contained 14.7 somatic protein-altering SNVs and indels (Supplementary Table 4). Notably, adults (age of >15 years) showed 2.5 times more somatic protein-altering mutations than children (21.0 versus 8.2; $P < 0.0001$), and there was a clear correlation between the age of the affected individual and mutation number (Fig. 1a,b and Supplementary Fig. 2). However, disease outcome was not linked to mutation number (Supplementary Fig. 3). Notably, a larger fraction of somatic SNVs in adults were cytosine-to-thymine transitions, and adults had a lower fraction of adenine-to-guanine transitions than children (Fig. 1c,d).

Protein-altering mutations occurred across 508 genes (Supplementary Table 5). To distinguish driver mutations from passenger ones, we only considered genes that were mutated in at least two samples and were significantly more mutated than the local background mutation rate, as calculated by Genome MuSiC[10] (Supplementary Table 6). We identified 15 candidate driver genes meeting these two criteria (Fig. 2 and Table 1) and 11 additional genes that were recurrently but not significantly mutated (Supplementary Fig. 4). Of the 15 candidate driver genes, 8 were known drivers in T-ALL, and 7 were new. Reassuringly, we found further mutations in many of the 15 candidate driver genes across

the 28 additional diagnosis samples and 17 cell lines that were sequenced (Fig. 2, Supplementary Fig. 5 and Supplementary Table 7).

Adult samples showed 2.7 times more mutations in candidate driver genes than children (1.9 versus 0.7; $P = 0.0034$) (Supplementary Fig. 2). Moreover, mutations in *FBXW7, CNOT3, PHF6, KDM6A* and *MAGEC3* were mainly present in adults, whereas *RPL10* mutations were almost exclusively found in children (Figs. 2 and 3, Table 1 and Supplementary Tables 8–10). Notably, our list of candidate driver genes included *RPL5* and *RPL10*, two genes encoding ribosomal proteins that occupy neighboring positions in the 60S ribosomal complex (Supplementary Fig. 6), with five exome samples carrying the same somatic mutation encoding a p.Arg98Ser alteration in RPL10. Also, the *CNOT3* gene showed evidence of a mutational hotspot, with three affected individuals carrying a substitution at Arg57 (Fig. 3a). Screening for mutations in these 3 genes in an independent confirmation cohort of 144 T-ALLs identified additional mutations in each of these genes (Fig. 3a and Supplementary Tables 8 and 9), resulting in total mutation frequencies of 3.8% (8/211) for *CNOT3* and 7.1% (15/211) for *RPL5* and *RPL10*. Adding the results from the confirmation cohort consolidated the association between *CNOT3* mutations and adult age ($P = 0.01$), and *CNOT3* was found to be mutated in 7 of 89 (7.9%) adult T-ALLs. In contrast, *RPL10* mutations were associated with young age ($P = 0.03$), and 10 of 122 (8.2%) pediatric cases had *RPL10* mutations (Fig. 3b). Mutations in *CNOT3, RPL10* or *RPL5* were not associated with any of the major molecular subgroups in T-ALL or with *NOTCH1* mutations (Supplementary Tables 8–10).

Ribosomal defects have been identified in inherited hematopoietic disorders (called ribosomopathies) that result in anemia and a propensity to develop leukemia[11]. Mutations in *RPL5* have previously been associated with Diamond Blackfan anemia and were studied in much detail in that context[11], but mutation of *RPL10* has not been described in any disease. Notably, loss of RPL22, another 60S ribosomal protein, was also recently identified in T-ALL[12], and, in our exome cohort, we also detected one affected individual with a frameshift mutation in *RPL22* (Supplementary Table 5).

RPL10 is located on the X chromosome, and 7 of 11 mutant cases were males carrying the mutation in nearly all leukemia cells. Moreover, the single *RPL10*-mutated female from whom we had RNA available expressed only the mutant allele in tumor cells (Supplementary Fig. 7). To confirm that these *RPL10* mutations were not random passenger mutations but alter RPL10 function, we engineered yeast cells expressing wild-type Rpl10, Rpl10 Arg98Ser, Rpl10 Arg98Cys or Rpl10 His123Pro as the sole copy of Rpl10. Rpl10 has been intensively studied[13] and is highly conserved in yeast, with Arg98 being unchanged from yeast to humans (Supplementary Fig. 8a). Notably, the Arg98 and His123 residues are closely apposed in a β hairpin near the peptidyltransferase center, the catalytic core of the ribosome (Supplementary Fig. 8b,c). In yeast, expression of the Rpl10 mutants impaired proliferation and caused a ribosome biogenesis defect, evidenced by the altered ratio of mature 80S to free subunits and the reduced presence of polysomes (Fig. 4a,b and Supplementary Fig. 9). In addition, Nmd3 and Tif6 showed aberrant accumulation in the cytoplasm in cells expressing Rpl10 Arg98Ser (Fig. 4c and Supplementary Fig. 9), indicating that this alteration impaired the release of the 60S export adaptor Nmd3 as well as

the subunit anti-association factor Tif6. The deleterious effects of the Rpl10 mutants were partially suppressed by expressing Nmd3 Leu291Phe (Fig. 4d), a mutant with weakened affinity for the ribosome[14], and by increasing the dosage of the *Nmd3* gene (Supplementary Fig. 9). These data indicate that the Rpl10 mutants affect the release of Nmd3 from the ribosome. Retention of Nmd3 and Tif6 on pre-60S subunits blocks ribosome assembly, and the resulting depletion of Nmd3 from the nucleus reduces the export of new ribosome subunits[15]. We also tested the effect of the expression of human RPL10 Arg98Ser, the most frequent RPL10 alteration, in lymphoid cells. In these cells, expression of RPL10 Arg98Ser also resulted in proliferation and ribosome biogenesis defects (Fig. 4e,f).

In the context of *CNOT3*, some of the mutations we identified were clearly truncating, whereas another group of mutations seemed to represent missense mutations affecting Arg57. Analysis of mRNA expression, however, showed that, also in the cases with Arg57 alteration, the mutant transcripts were not or were only weakly expressed (Supplementary Fig. 7). This is most likely caused by splicing defects, as the mutations are located at the splice donor site of exon 5. The mutations in *CNOT3* thus suggest that this gene acts as a tumor suppressor in T-ALL. CNOT3 is part of the CCR4-NOT complex that regulates gene expression transcriptionally and post-transcriptionally[16]. Cnot3 also mediates self-renewal in mouse embryonic stem cells, where Cnot3 shares many target genes with Myc[17], a known oncogene in T-ALL. To investigate the effect of loss of CNOT3 in tumor formation, we used an established *Drosophila* eye cancer model. We used the sensitized model in which the Notch ligand Delta is overexpressed in the developing eyes. These flies have larger eyes but by themselves do not develop tumors[3,7,18,19], and this model is relevant for T-ALL, given the central role of NOTCH1 signaling in this disease[1]. Reduction of *Not3* expression in this genetic background resulted in a marked increase in tumor incidence from 8% of the eyes with control RNA interference (RNAi) to 46% up to 90% with three different *Not3* RNAi lines and one line with a P-element insertion in *Not3* (Fig. 5). These data support the notion that reduction in *Not3* expression is sufficient to transform sensitized cells.

Using whole-exome sequencing, we describe clear differences between pediatric and adult T-ALL and identify a spectrum of driver mutations that function in various cellular processes. One notable observation is that a subset of T-ALL cases have accumulated mutations that affect the function of the ribosome, and it is currently unclear what advantage this might provide to the cancer cells. This is, however, very similar to recent findings of deregulated splicing in myelodysplasia and chronic lymphocytic leukemia[20–23] and might indicate that cancer cells have mechanisms to overcome defects in these basic processes. Indeed, cancer cells might compensate for the deleterious effects of mutations affecting the ribosome by acquiring additional mutations, similar to the suppressive effect of the Nmd3 Leu291Phe alteration that we describe in the yeast model (Fig. 4d). Alternatively, the mutations affecting the ribosome might downregulate the hyperactive translation machinery in cancer cells[24], which could be beneficial for the fitness of these cells. Our data shed light on the diversity of mutations that are implicated in T-ALL development and on the differences between adult and pediatric T-ALL.

ONLINE METHODS

Leukemia samples and cell lines

T-ALL samples were collected at various institutions. All patients gave their informed consent, and all samples were obtained according to the guidelines of the local ethical committees. This study was approved by the ethical committee of the University Hospital Leuven. The Ba/F3 mouse pro-B-cell line and all human T-ALL cell lines were obtained from Deutsche Sammlung von Mikroorganismen und Zellkulturen (DSMZ).

Sequencing

Genomic DNA samples from affected individuals and cell lines were sonicated to give a fragment size of 250 bp on a Bioruptor UCD-300 instrument (Diagenode). Library preparation was carried out using the Truseq DNA sample prep kit (Illumina), and capture was performed with SeqCapEZ Exome v2.0 (Nimblegen) or Agilent SureSelect 38 Mb (Agilent) capture reagents. Captured samples were sequenced on a HiSeq 2000 (Illumina) operated in paired-end 2 × 100 bp mode. Reads from each sample were aligned to the reference genome version hg19 using the Burrows-Wheeler Aligner (BWA)[52]. Alignment files were processed further with the Genome Analysis Toolkit (GATK) before variant calling. Duplicate removal, local realignment around known indels and base quality recalibration were performed as described elsewhere[53]. Variants were called using the variant quality score recalibration (VQSR) protocol in GATK. Variant calling was performed for each sample separately, and somatic variants were identified by selecting the variants observed at diagnosis that were absent at remission. The somatic score for each variant was calculated with the Somatic Sniper[54] algorithm using the processed alignment files for diagnosis and remission samples. Indel calling was performed with DINDEL[55] using the calibrated bam files for each sample separately. Somatic indel detection was performed by identifying the high-quality indels in the diagnosis sample (minimum read depth of 15 at the variant site and 15% of the reads supporting the variant allele) and then filtering out the ones observed in the corresponding remission sample (minimum read depth of 1).

Sanger validation of results

All predicted somatic variants shown in Figure 2 were tested and confirmed by conventional Sanger sequencing. These and additional SNVs and indels validated by Sanger sequencing are reported in Supplementary Tables 5 and 7. Overall, we performed Sanger sequencing validation for 219 SNVs, of which 202 were confirmed (92.2% validation rate), and of 78 indels, of which 61 were confirmed (78% validation rate). Analysis of the chromatograms from Sanger sequencing was performed using CLC Main Workbench 6 (CLC Bio). Predicted somatic variants that were not confirmed by Sanger sequencing are not shown in Figure 2 but are reported in Supplementary Table 5 and are indicated as false positives. The entire coding sequences of the *RPL5, RPL10* and *CNOT3* genes were PCR amplified, and Sanger sequencing was performed on whole-genome amplified DNA from an independent set of 144 individuals with T-ALL. Primer sequences are provided in Supplementary Table 11. Mutation detection was performed using Mutation Surveyor v4.0.4 (Softgenetics). Detected variants were confirmed on original, non-amplified material and were tested for their somatic origin using DNA from remission samples, if available.

Statistical testing

Throughout this study, statistical significance was defined as $P < 0.05$. The statistical testing methods used are described in the figure and table legends.

Drosophila experiments

The fly line 15271 (*y*^{1}; *P*{*SUPor-P*}*l*(*2*)*NC136*^{KG10496}/*CyO*; *ry*^{506}) with a P-element insertion in the *Not3* gene was obtained from the Bloomington Stock Center[56]. *Not3* RNAi fly lines v37547 (*w1118*; *P*{*GD4068*}*v37547*), v37545 (*w1118*; *P*{*GD4068*}*v37545*) and v105990 (*w1118*; *P*{*KK102144*}*VIE-260B*) were purchased from the Vienna *Drosophila* RNAi Center (VDRC)[57]. Control RNAi flies (*w*; *Sp*/*CyO*; *UAS-w dsRNA*) and the Cy8 sensitized fly (*w*; *eyeless-Gal4*; *UAS-Dl*/*CyO*) were described previously[3]. All fly strains were crossed to Cy8 virgin females. From the performed crosses, the F_1 progeny obtained with the following genotypes were selected: Cy8 × 15271 (*eyeless-Gal4*; *UAS-Dl*/*P*{*SUPor-P*}*l*(*2*)*NC136*^{KG10496}; *ry*^{506}/+), Cy8 × v37547 (*eyeless-Gal4*; *UAS-Dl*/+; *P*{*GD4068*}*v37547*/+), Cy8 × v37545 (*eyeless-Gal4*; *UAS-Dl*/+; *P*{*GD4068*}*v37545*/+), Cy8 × v105990 (*eyeless-Gal4*; *UAS-Dl*; *P*{*KK102144*}*VIE-260B*) and Cy8 × control (*eyeless-Gal4*; *UAS-Dl*/*CyO*; *UAS-w dsRNA*/+).

All flies were raised at 25 °C on standard fly food. To analyze the tumor burden, each eye was scored separately in the selected F_1 progeny. Eyes were counted as hyperplastic when the eye showed at least one fold.

Yeast experiments

Codon 98 of yeast (*Saccharomyces cerevisiae*) *RPL10* in the centromeric *LEU2* vector pAJ2522 was changed from AGA to either TCT or TGT, and codon 123 was changed from CAC to CCA by site-specific mutagenesis. Wild-type and mutant constructs were introduced into the *Rpl10* deletion strain AJY1437 (*MATα rpl10*::*KanMX lys2Δ0 met15Δ0 his3Δ1 leu2Δ0 ura3Δ0* pAJ392 - *Rpl10 URA3 CEN*) by plasmid shuffle or the conditional glucose-repressible *Rpl10* strain AJY3373 (*MATα KanMX-GAL1-RPL10 his3Δ1 leu2Δ0 ura3Δ0*) and assayed for growth by plating tenfold serial dilutions onto selective medium. To test suppression of Rpl10 mutants by mutations in *Nmd3*, empty vector or vector expressing wild-type Nmd3 or Nmd3 Leu291Phe was introduced into the indicated strains.

Polysome profiles were analyzed as described[2]. Constructs expressing wild-type *Rpl10* or *Rpl10* mutants were introduced into AJY1837, which contains a glucose-repressible *Rpl10* gene (*GAL-Rpl10*), the LMB-sensitive *Crm1* allele encoding the Thr539Cys variant and *Nmd3-GFP*, and AJY2766, containing *GAL-Rpl10* and *Tif6-GFP*. Cultures were grown in selective medium containing galactose. Glucose was added to repress the expression of wild-type genomic *Rpl10* for 2 h, and LMB was added to a final concentration of 0.1 μg/ml for 30 min to block Nmd3 shuttling. Images were captured using a Nikon E800 microscope fitted with a 100× Plan Apo objective and a Photometrics CoolSNAP ES camera controlled by NIS-Elements AR 2.10 software. Images were prepared using Adobe Photoshop 7.0.

Experiments in mammalian cells

Wild-type *RPL10* cDNA (ENST00000344746) was PCR amplified from human thymus cDNA and cloned into the BglII and EcoRI sites of pMSCV-GFP. The mutation encoding the p.Arg98Ser alteration was introduced by mutagenesis of the wild-type *RPL10* construct. Mouse lymphoid pro-B cells (Ba/F3) were transduced with pMSCV retroviral constructs expressing wild-type RPL10 or the Arg98Ser mutant according to standard methods. To mimic the situation in individuals with T-ALL, where only mutant and not wild-type RPL10 is expressed in leukemia cells (Supplementary Fig. 7), Ba/F3 cell experiments were performed with concurrent knockdown of endogenous *Rpl10*. Delivery of small interfering RNA (siRNA) into the cells was performed by electoporation on a Gene Pulser Xcell machine (Bio-Rad) using exponential decay, 250 V and 950 μF. siRNAs against mouse *Rpl10* were used at a concentration of 400 nM during electroporation and were obtained from Integrated DNA Technologies (IDT). Cell proliferation was measured on a Guava flow cytometer (Millipore) at the indicated time points after electroporation.

For polysome profiling, Ba/F3 cells were homogenized in a solution with 100 mM Tris-HCl, pH 7.5, 100 mM NaCl, 100 mM $MgCl_2$, 1% DOC/Triton X-100, 1 mM dithiothreitol, 10 μl/ml Protease Inhibitor Cocktail (Sigma), 10 μl/ml Phosphatase Inhibitor Cocktail I (Sigma), 10 μl/ml Phosphatase Inhibitor Cocktail II (Sigma) and 30 U/ml RNasin supplemented with 100 μg/ml cycloheximide. After 5 min of incubation on ice, the extract was centrifuged for 5 min at 12,000 g at 4 °C. The supernatant was loaded onto a 10–60% sucrose gradient and sedimented by centrifugation at 4 °C for 150 min at 37,000 rpm in a Beckman SW41 rotor.

Supplementary Material

Refer to Web version on PubMed Central for supplementary material.

Acknowledgments

This work was supported by grants from KU Leuven (concerted action grant to J. Cools and P.V. and PF/10/016 SymBioSys to J. Cools and S.A.), FWO-Vlaanderen (G.0546.11 to J. Cools, P.V., S.A. and A.U. and G.0704.11N to S.A.), the Foundation against Cancer (SCIE2006-34 to J. Cools and 2010-154 to S.A.), a European Research Council (ERC) starting grant (J. Cools), the Interuniversity Attraction Poles (IAP) granted by the Federal Office for Scientific, Technical and Cultural Affairs, Belgium (J. Cools and P.V.), a grant from the Ministry of Health, Cancer Plan (J. Cools, P.V. and S.A.), a grant from the French program Carte d'Identité des Tumeurs (CIT, Ligue Contre le Cancer) and from Cancéropole d'Ile de France (J.S.), and a grant from the US National Institutes of Health (NIH; GM53655 to A.W.J. and S.P.). K.D.K. is a postdoctoral researcher, and P.V. is a senior clinical investigator of FWO-Vlaanderen.

References

1. Grabher C, von Boehmer H, Look AT. Notch 1 activation in the molecular pathogenesis of T-cell acute lymphoblastic leukaemia. Nat. Rev. Cancer. 2006; 6:347–359. [PubMed: 16612405]
2. Van Vlierberghe P, Ferrando A. The molecular basis of T cell acute lymphoblastic leukemia. J. Clin. Invest. 2012; 122:3398–3406. [PubMed: 23023710]
3. Ferres-Marco D, et al. Epigenetic silencers and Notch collaborate to promote malignant tumours by *Rb* silencing. Nature. 2006; 439:430–436. [PubMed: 16437107]
4. De Keersmaecker K, Marynen P, Cools J. Genetic insights in the pathogenesis of T-cell acute lymphoblastic leukemia. Haematologica. 2005; 90:1116–1127. [PubMed: 16079112]

5. Pui CH, Relling MV, Downing JR. Acute lymphoblastic leukemia. N. Engl. J. Med. 2004; 350:1535–1548. [PubMed: 15071128]
6. Homminga I, et al. Integrated transcript and genome analyses reveal *NKX2*-1 and *MEF2C* as potential oncogenes in T cell acute lymphoblastic leukemia. Cancer Cell. 2011; 19:484–497. [PubMed: 21481790]
7. Ntziachristos P, et al. Genetic inactivation of the polycomb repressive complex 2 in T cell acute lymphoblastic leukemia. Nat. Med. 2012; 18:298–301. [PubMed: 22237151]
8. Zhang J, et al. The genetic basis of early T-cell precursor acute lymphoblastic leukaemia. Nature. 2012; 481:157–163. [PubMed: 22237106]
9. Larson DE, et al. SomaticSniper: identification of somatic point mutations in whole genome sequencing data. Bioinformatics. 2012; 28:311–317. [PubMed: 22155872]
10. Dees ND, et al. MuSiC: identifying mutational significance in cancer genomes. Genome. Res. 2012; 22:1589–1598. [PubMed: 22759861]
11. Narla A, Ebert BL. Ribosomopathies: human disorders of ribosome dysfunction. Blood. 2010; 115:3196–3205. [PubMed: 20194897]
12. Rao S, et al. Inactivation of ribosomal protein L22 promotes transformation by induction of the stemness factor, Lin28B. Blood. 2012; 120:3764–3773. [PubMed: 22976955]
13. Hofer A, Bussiere C, Johnson AW. Mutational analysis of the ribosomal protein Rpl10 from yeast. J. Biol. Chem. 2007; 282:32630–32639. [PubMed: 17761675]
14. Hedges J, et al. Release of the export adapter, Nmd3p, from the 60S ribosomal subunit requires Rpl10p and the cytoplasmic GTPase Lsg1p. EMBO J. 2005; 24:567–579. [PubMed: 15660131]
15. Lo KY, et al. Defining the pathway of cytoplasmic maturation of the 60S ribosomal subunit. Mol. Cell. 2010; 39:196–208. [PubMed: 20670889]
16. Collart MA, Panasenko OO. The Ccr4-not complex. Gene. 2012; 492:42–53. [PubMed: 22027279]
17. Hu G, et al. A genome-wide RNAi screen identifies a new transcriptional module required for self-renewal. Genes. Dev. 2009; 23:837–848. [PubMed: 19339689]
18. Palomero T, et al. Mutational loss of PTEN induces resistance to NOTCH1 inhibition in T-cell leukemia. Nat. Med. 2007; 13:1203–1210. [PubMed: 17873882]
19. Bossuyt W, et al. The atonal proneural transcription factor links differentiation and tumor formation in *Drosophila*. PLoS Biol. 2009; 7:e40. [PubMed: 19243220]
20. Quesada V, et al. Exome sequencing identifies recurrent mutations of the splicing factor *SF3B1* gene in chronic lymphocytic leukemia. Nat. Genet. 2012; 44:47–52.
21. Graubert TA, et al. Recurrent mutations in the *U2AF1* splicing factor in myelodysplastic syndromes. Nat. Genet. 2012; 44:53–57.
22. Yoshida K, et al. Frequent pathway mutations of splicing machinery in myelodysplasia. Nature. 2011; 478:64–69. [PubMed: 21909114]
23. Papaemmanuil E, et al. Somatic *SF3B1* mutation in myelodysplasia with ring sideroblasts. N. Engl. J. Med. 2011; 365:1384–1395. [PubMed: 21995386]
24. Ruggero D, Pandolfi PP. Does the ribosome translate cancer? Nat. Rev. Cancer. 2003; 3:179–192. [PubMed: 12612653]
25. Weng AP, et al. Activating mutations of *NOTCH1* in human T cell acute lymphoblastic leukemia. Science. 2004; 306:269–271. [PubMed: 15472075]
26. Fabbri G, et al. Analysis of the chronic lymphocytic leukemia coding genome: role of *NOTCH1* mutational activation. J. Exp. Med. 2011; 208:1389–1401. [PubMed: 21670202]
27. Puente XS, et al. Whole-genome sequencing identifies recurrent mutations in chronic lymphocytic leukaemia. Nature. 2011; 475:101–105. [PubMed: 21642962]
28. Westhoff B, et al. Alterations of the Notch pathway in lung cancer. Proc. Natl. Acad. Sci. USA. 2009; 106:22293–22298. [PubMed: 20007775]
29. Agrawal N, et al. Exome sequencing of head and neck squamous cell carcinoma reveals inactivating mutations in *NOTCH1*. Science. 2011; 333:1154–1157. [PubMed: 21798897]
30. Stransky N, et al. The mutational landscape of head and neck squamous cell carcinoma. Science. 2011; 333:1157–1160. [PubMed: 21798893]

31. Robinson DR, et al. Functionally recurrent rearrangements of the MAST kinase and Notch gene families in breast cancer. Nat. Med. 2011; 17:1646–1651. [PubMed: 22101766]
32. Jiao X, et al. Somatic mutations in the Notch, NF-κB, PIK3CA, and Hedgehog pathways in human breast cancers. Genes Chromosom. Cancer. 2012; 51:480–489. [PubMed: 22302350]
33. Thompson BJ, et al. The SCFFBW7 ubiquitin ligase complex as a tumor suppressor in T cell leukemia. J. Exp. Med. 2007; 204:1825–1835. [PubMed: 17646408]
34. Welcker M, Clurman BE. FBW7 ubiquitin ligase: a tumour suppressor at the crossroads of cell division, growth and differentiation. Nat. Rev. Cancer. 2008; 8:83–93. [PubMed: 18094723]
35. Tosello V, et al. *WT1* mutations in T-ALL. Blood. 2009; 114:1038–1045. [PubMed: 19494353]
36. King-Underwood L, Pritchard-Jones K. Wilms' tumor (*WT1*) gene mutations occur mainly in acute myeloid leukemia and may confer drug resistance. Blood. 1998; 91:2961–2968. [PubMed: 9531607]
37. De Keersmaecker K, et al. The *TLX1* oncogene drives aneuploidy in T cell transformation. Nat. Med. 2010; 16:1321–1327. [PubMed: 20972433]
38. Klauck SM, et al. Mutations in the ribosomal protein gene *RPL10* suggest a novel modulating disease mechanism for autism. Mol. Psychiatry. 2006; 11:1073–1084. [PubMed: 16940977]
39. Chiocchetti A, et al. Mutation and expression analyses of the ribosomal protein gene *RPL10* in an extended German sample of patients with autism spectrum disorder. Am. J. Med. Genet. A. 2011; 155:1472–1475.
40. Kalender Atak Z, et al. High accuracy mutation detection in leukemia on a selected panel of cancer genes. PLoS ONE. 2012; 7:e38463. [PubMed: 22675565]
41. Durieux AC, Prudhon B, Guicheney P, Bitoun M. Dynamin 2 and human diseases. J. Mol. Med. 2010; 88:339–350. [PubMed: 20127478]
42. Van Vlierberghe P, et al. *PHF6* mutations in T-cell acute lymphoblastic leukemia. Nat. Genet. 2010; 42:338–342. [PubMed: 20228800]
43. Van Vlierberghe P, et al. *ETV6* mutations in early immature human T cell leukemias. J. Exp. Med. 2011; 208:2571–2579. [PubMed: 22162831]
44. Lower KM, et al. 1024C>T (R342X) is a recurrent *PHF6* mutation also found in the original Börjeson-Forssman-Lehmann syndrome family. Eur. J. Hum. Genet. 2004; 12:787–789. [PubMed: 15241480]
45. Ono R, et al. LCX, leukemia-associated protein with a CXXC domain, is fused to MLL in acute myeloid leukemia with trilineage dysplasia having t(10;11)(q22;q23). Cancer. Res. 2002; 62:4075–4080. [PubMed: 12124344]
46. Lorsbach RB, et al. TET1, a member of a novel protein family, is fused to MLL in acute myeloid leukemia containing the t(10;11)(q22;q23). Leukemia. 2003; 17:637–641. [PubMed: 12646957]
47. Burmeister T, et al. The MLL recombinome of adult CD10-negative B-cell precursor acute lymphoblastic leukemia: results from the GMALL study group. Blood. 2009; 113:4011–4015. [PubMed: 19144982]
48. van Haaften G, et al. Somatic mutations of the histone H3K27 demethylase gene *UTX* in human cancer. Nat. Genet. 2009; 41:521–523. [PubMed: 19330029]
49. Gui Y, et al. Frequent mutations of chromatin remodeling genes in transitional cell carcinoma of the bladder. Nat. Genet. 2011; 43:875–878. [PubMed: 21822268]
50. Lederer D, et al. Deletion of KDM6A, a histone demethylase interacting with MLL2, in three patients with Kabuki syndrome. Am. J. Hum. Genet. 2012; 90:119–124. [PubMed: 22197486]
51. Pasqualucci L, et al. Analysis of the coding genome of diffuse large B-cell lymphoma. Nat. Genet. 2011; 43:830–837. [PubMed: 21804550]
52. Li H, Durbin R. Fast and accurate short read alignment with Burrows-Wheeler transform. Bioinformatics. 2009; 25:1754–1760. [PubMed: 19451168]
53. DePristo MA, et al. A framework for variation discovery and genotyping using next-generation DNA sequencing data. Nat. Genet. 2011; 43:491–498. [PubMed: 21478889]
54. Larson DE, et al. SomaticSniper: identification of somatic point mutations in whole genome sequencing data. Bioinformatics. 2012; 28:311–317. [PubMed: 22155872]

55. Albers CA, et al. Dindel: accurate indel calls from short-read data. Genome. Res. 2011; 21:961–973. [PubMed: 20980555]

56. Bellen HJ, et al. The BDGP gene disruption project: single transposon insertions associated with 40% of *Drosophila* genes. Genetics. 2004; 167:761–781. [PubMed: 15238527]

57. Dietzl G, et al. A genome-wide transgenic RNAi library for conditional gene inactivation in *Drosophila*. Nature. 2007; 448:151–156. [PubMed: 17625558]

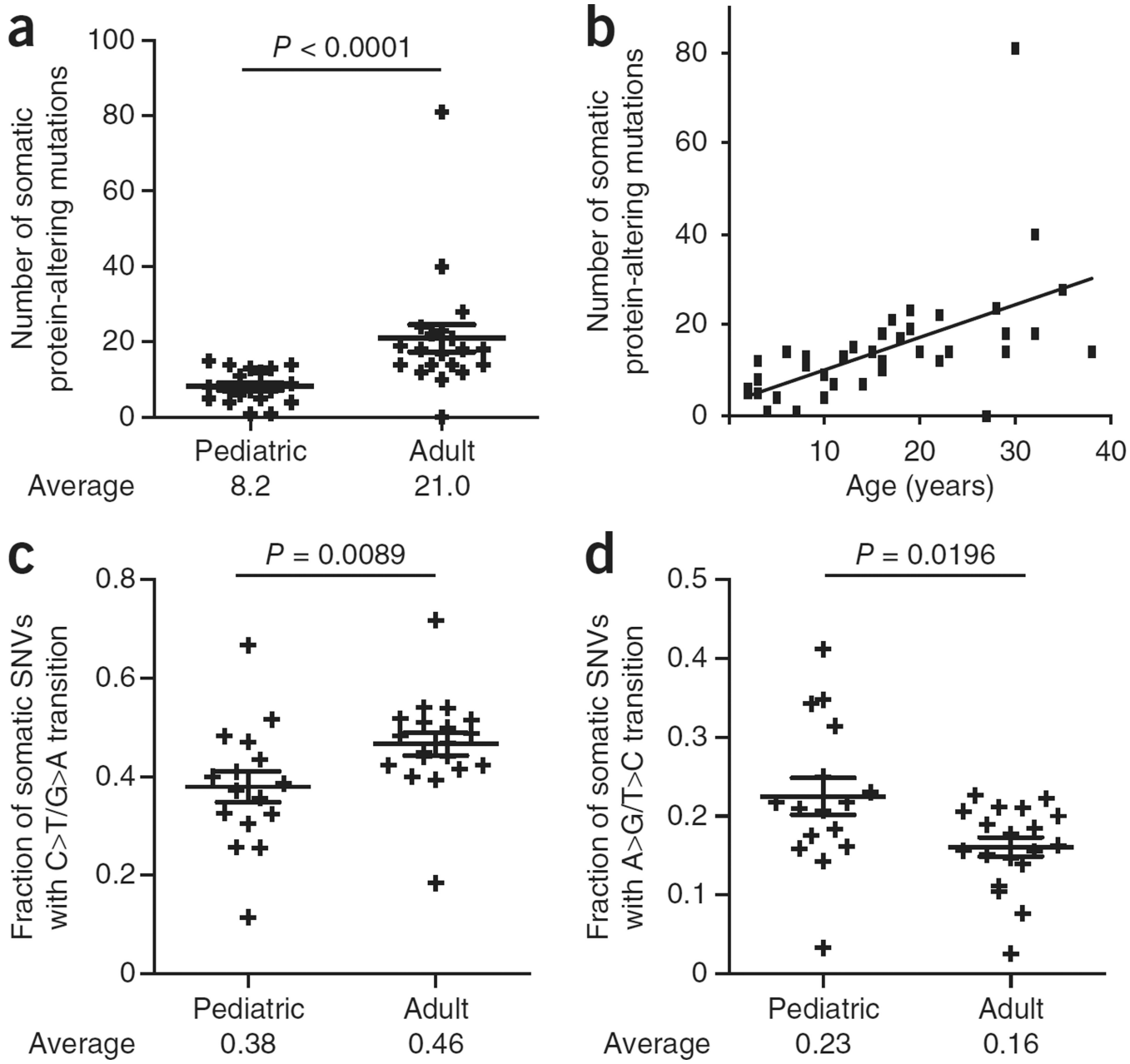

Figure 1.

Correlation between the age of the affected individual and mutation number and type. (**a**) Plot showing the number of protein-altering somatic mutations in pediatric (≤15 years) and adult (≥16 years) individuals with T-ALL. Averages and s.e.m. are shown. The *P* value tested whether there was a significantly different mutation number in adults versus children and was calculated using the two-tailed Wilcoxon signed-rank test. Pediatric cases, $n = 19$; adult cases, $n = 20$. (**b**) Dot plot representing the number of protein-altering somatic mutations versus age of the affected individual. (**c,d**) Plots showing the fraction of somatic SNVs that were C>T/G>A transitions (c) or A>G/*T*>C transitions (**d**) in pediatric and adult individuals with T-ALL. Averages and s.e.m. are shown. Samples with fewer than ten

somatic SNVs were excluded from this analysis. The reported *P* values test whether there was a significant difference between adults and children and was calculated using the two-tailed Wilcoxon signed-rank test. Pediatric cases, $n = 16$; adult cases, $n = 19$.

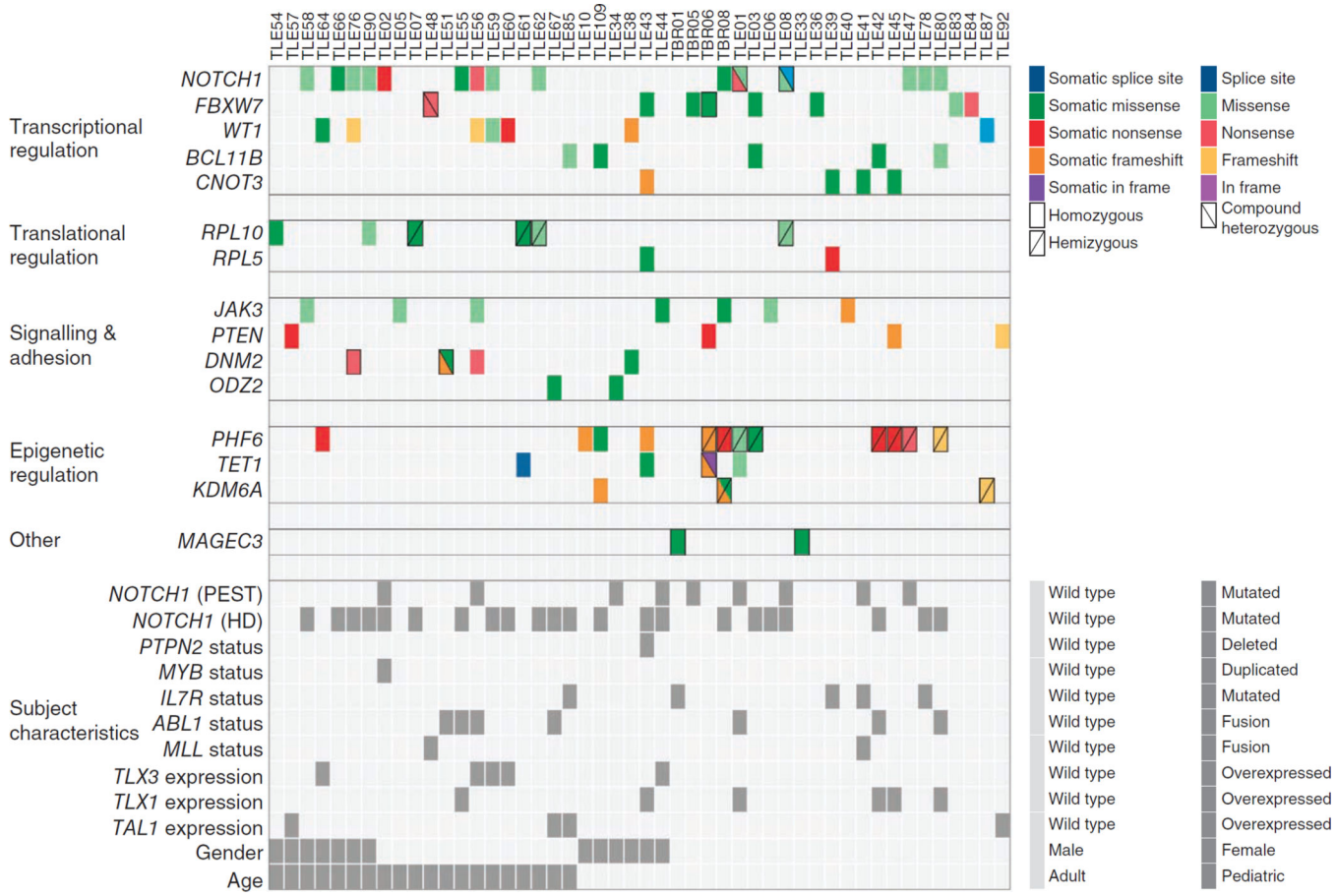

Figure 2.

Overview of mutations in 15 identified candidate T-ALL driver genes in 67 samples from affected individuals. Top, mutations in 15 candidate T-ALL driver genes are shown across the set of cases. For clarity, only affected individuals harboring mutations in at least 1 of the 15 genes are included. Each type of mutation is indicated by color, and symbols indicate whether the mutation was homozygous, hemizygous or compound heterozygous. Mutations with no indication are heterozygous. All mutations shown here were validated by Sanger sequencing. Bottom, the characteristics of the relevant individuals (identified by Sanger sequencing, karyotyping or gene expression analysis) are shown. Mutations in *NOTCH1* were hard to identify by exome sequencing owing to low capture efficiency and resulting low sequence coverage of *NOTCH1*. Detailed descriptions of the mutations shown in this figure are provided in Supplementary Tables 5 and 7–9.

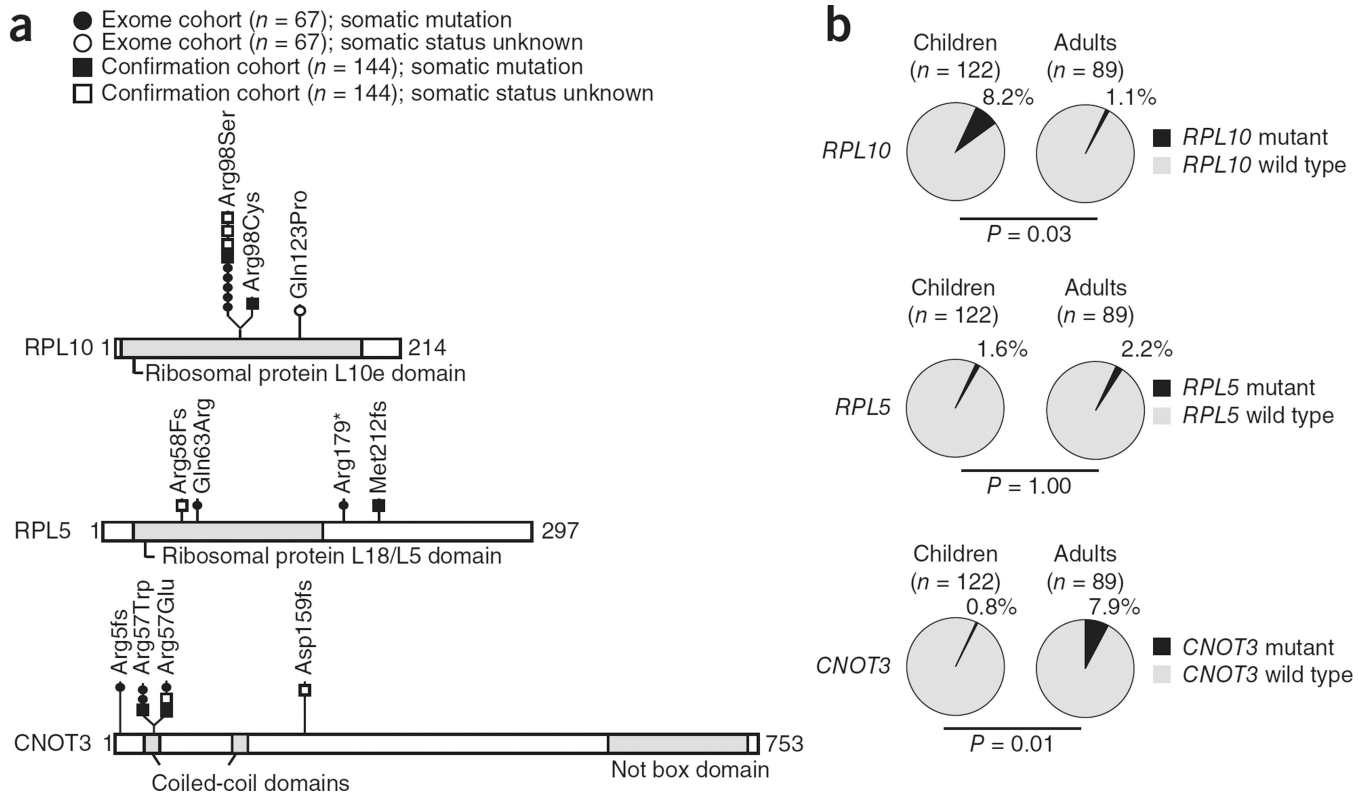

Figure 3.

Overview of mutations in *RPL10, RPL5* and *CNOT3*. (**a**) Schematics of RPL10, RPL5 and CNOT3 protein structures with the positions of the alterations detected in 211 T-ALL samples indicated. The somatic status of the mutations is indicated. The characteristics of the individuals with *RPL10, RPL5* or *CNOT3* mutations are reported in Supplementary Tables 8 and 9. (**b**) Pie charts reporting mutation frequencies detected in adult versus pediatric individuals with T-ALL. All reported *P* values tested whether there was a significant difference in mutation frequency in adults versus children and were calculated using the unpaired *t* test.

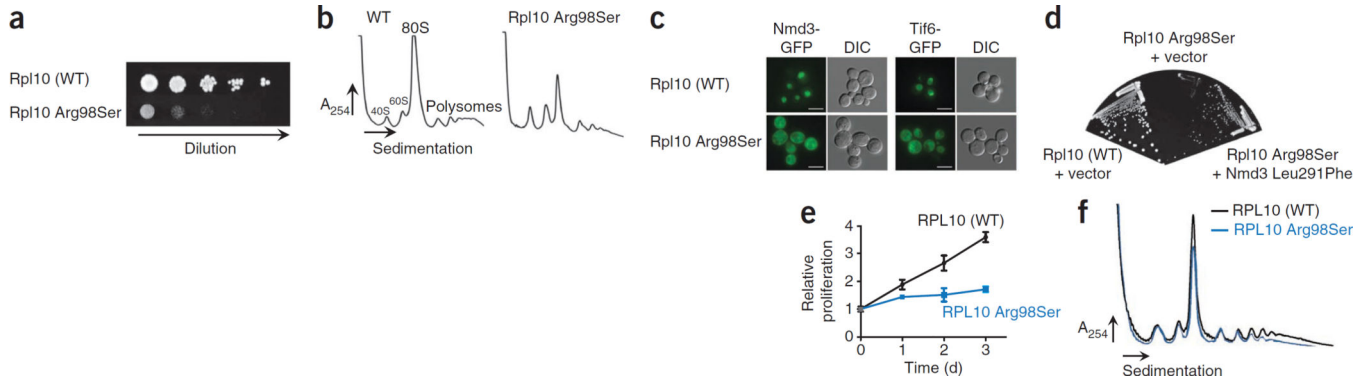

Figure 4.

Cellular effects of the RPL10 p.Arg98Ser alteration. (**a,b**) The growth of yeast cells expressing wild-type (WT) Rpl10 or Rpl10 Arg98Ser was compared by plating tenfold serial dilutions (**a**), and polysome profiles were obtained (**b**). A_{254}, absorbance at 254 nm. (**c**) The fluorescence of Nmd3-GFP and Tif6-GFP was examined in cells expressing wild-type Rpl10 or Rpl10 Arg98Ser. Scale bars, 5 μm. DIC, differential interference contrast. In the case of Nmd3, cells also contained leptomycin B (LMB)-sensitive Crm1, and Nmd3-GFP localization was examined after treatment with LMB to trap Nmd3 in the nucleus. (**d**) Yeast cells expressing wild-type Rpl10 or Rpl10 Arg98Ser were transformed with empty vector or vector expressing Nmd3 Leu291Phe. Tenfold serial dilutions were grown. (**e**) Proliferation curves of mouse B cells (Ba/F3) expressing wild-type RPL10 or RPL10 Arg98Ser. Error bars, s.d. of measurements in triplicate. (**f**) Polysome profiling in Ba/F3 cells expressing human wild-type RPL10 or RPL10 Arg98Ser.

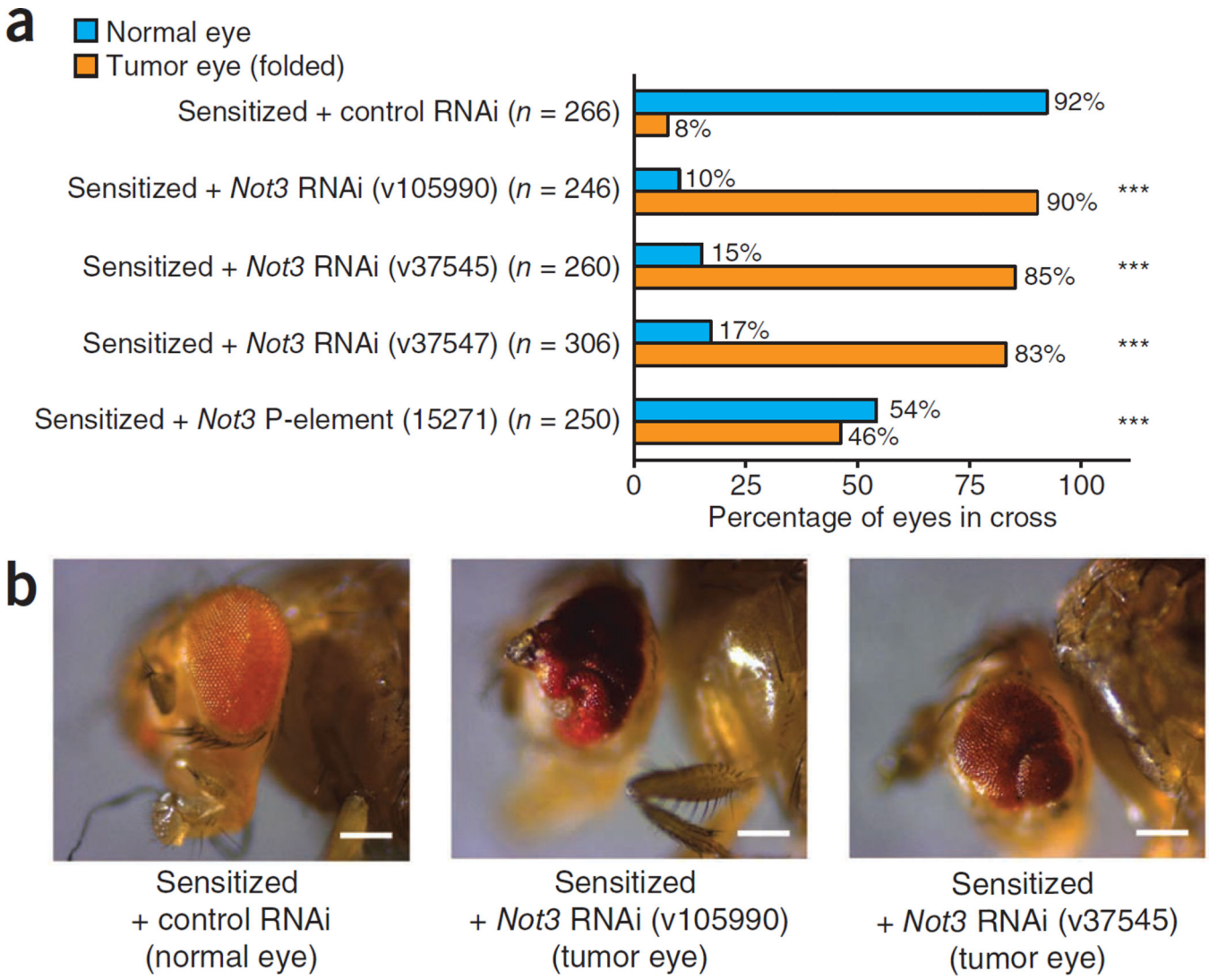

Figure 5.

Reduced *Not3* expression promotes tumor development in a *Drosophila* sensitized background. (**a,b**) Sensitized flies overexpressing the Notch ligand Delta in the eye were crossed to one of three different *Drosophila Not3* RNAi fly lines (v105990, v37545, v37547), to the 15271 line with a P-element insertion in *Not3* or to control RNAi flies (with an RNAi construct against the *white* (*w*) gene). Shown are quantitative (**a**) and qualitative (**b**) representations of the eye tumor burden in different genotypes. ***, tumor incidence in this cross was significantly different from that in the control cross ($P < 0.001$) as analyzed by two-tailed Fisher's exact test. Scale bars in **b**, 200 μm.

Table 1

Significantly and recurrently mutated genes in T-ALL

Gene	Number of subjects with mutations	Gene function	Associated age group	Associated pathologies with genomic alterations
NOTCH1	29/67 (43.3%)[a]	Transmembrane receptor, releases intracellular NOTCH1 transcriptional enhancer upon activation	None	T-ALL[25], CLL[26,27], lung cancer[28], head and neck cancer[29,30], breast cancer[31,32]
FBXW7	8/67 (11.9%)	Part of ubiquitin ligase complex targeting cyclin E, MYC and NOTCH1	None	T-ALL[33], various cancer types[34]
WT1	7/67 (10.4%)	Zinc-finger transcription factor	None	T-ALL[35], AML[36], Wilms tumor
BCL11B	5/67 (7.5%)	Zinc-finger transcription factor	None	T-ALL[37]
CNOT3	8/211 (3.8%)	Part of the CCR4-NOT complex that regulates gene expression	Adult	
RPL10	11/211 (5.2%)	Ribosomal protein of the 60S ribosomal subunit	Pediatric	Autism[38,39]
RPL5	4/211 (1.9%)	Ribosomal protein of the 60S ribosomal subunit	None	Diamond Blackfan anemia[11]
JAK3	7/67 (10.4%)	Kinase involved in cytokine receptor signaling	None	T-ALL[8,40], various myeloid and lymphoid malignancies
PTEN	4/67 (6.0%)	Phosphatase antagonizing PI3K function	None	T-ALL[18], various cancer types
DNM2	4/67 (6.0%)	Microtubule-associated GTPase	None	T-ALL[8], Charcot-Marie-Tooth disease[41], centronuclear myopathy[41]
ODZ2	2/67 (3.0%)	May function as a cellular signal transducer	None	
PHF6	12/67 (17.9%)	Plant homeodomain-like finger (PHF) family protein that may regulate transcription	Adult	T-ALL[42], AML[43], Borjeson-Forssman-Lehmann syndrome[44]
TET1	4/67 (6.0%)	Epigenetic regulator converting methylcytosine (5mC) to 5-hydroxymethylcytosine (5-hmC)	None	t(10;11)(q22;23) (*MLL-TET1* fusion) in AML and B-ALL[45–47]
KDM6A	3/67 (4.5%)	Histone demethylase for Lys27 of histone H3	None	Various cancer types[48,49], Kabuki syndrome[50]
MAGEC3	2/67 (3.0%)	Gene function unknown, only expressed in normal testis and in various tumor types	None	Diffuse large B-cell lymphoma[51]

CLL, chronic lymphocytic leukemia; AML, acute myeloid leukemia; B-ALL, B-cell acute lymphoblastic leukemia.

[a]Mutations in *NOTCH1* were hard to identify by exome sequencing due to poor capture efficiency and resulting low sequence coverage of *NOTCH1*. The reported mutation number reflects *NOTCH1* mutations detected by complementary Sanger sequencing.